

Inference of interactions between players based on asynchronously updated evolutionary game data

Hong-Li Zeng(曾红丽), Bo Jing(景涛), Yu-Hao Wang(王于豪), and Shao-Meng Qin(秦绍萌)
Citation: Chin. Phys. B, 2023, 32 (**8**): 080201. DOI: 10.1088/1674-1056/acc7fd
Journal homepage: http://cpb.iphy.ac.cn; http://iopscience.iop.org/cpb
What follows is a list of articles you may be interested in

Inverse Ising techniques to infer underlying mechanisms from data

Hong-Li Zeng(曾红丽), Erik Aurell
Chin. Phys. B, 2020, 29 (**8**): 080201. DOI: 10.1088/1674-1056/ab8da6

Effects of the planarity and heterogeneity of networks on evolutionary two-player games

Xu-Sheng Liu(刘旭升), Zhi-Xi Wu(吴枝喜), Jian-Yue Guan(关剑月)
Chin. Phys. B, 2018, 27 (**12**): 120203. DOI: 10.1088/1674-1056/27/12/120203

Homotopic mapping solitary traveling wave solutions for the disturbed BKK mechanism physical model

Zhou Xian-Chun (周先春), Shi Lan-Fang (石兰芳), Han Xiang-Lin (韩祥临), Mo Jia-Qi (莫嘉琪)
Chin. Phys. B, 2014, 23 (**9**): 090204. DOI: 10.1088/1674-1056/23/9/090204

A class of asymptotic solution for the time delay wind field model of an ocean

Zhou Xian-Chun (周先春), Shi Lan-Fang (石兰芳), Mo Jia-Qi (莫嘉琪)
Chin. Phys. B, 2014, 23 (**4**): 040202. DOI: 10.1088/1674-1056/23/4/040202

Modified variational iteration method for an El Niño Southern Oscillation delayed oscillator

Cao Xiao-Qun(曹小群), Song Jun-Qiang(宋君强), Zhu Xiao-Qian(朱小谦), Zhang Li-Lun(张理论), Zhang Wei-Min(张卫民), and Zhao Jun(赵军)
Chin. Phys. B, 2012, 21 (**2**): 020203. DOI: 10.1088/1674-1056/21/2/020203

Inference of interactions between players based on asynchronously updated evolutionary game data

Hong-Li Zeng(曾红丽)[1], Bo Jing(景浡)[2], Yu-Hao Wang(王于豪)[1], and Shao-Meng Qin(秦绍萌)[3,†]

[1] *College of Science, Nanjing University of Posts and Telecommunications, Nanjing* 210023, *China*
[2] *College of Electronic Science and Engineering, Nanjing University of Posts and Telecommunications, Nanjing* 210046, *China*
[3] *College of Science, Civil Aviation University of China, Tianjin* 300300, *China*

(Received 29 December 2022; revised manuscript received 6 March 2023; accepted manuscript online 28 March 2023)

The interactions between players of the prisoner's dilemma game are inferred using observed game data. All participants play the game with their counterparts and gain corresponding rewards during each round of the game. The strategies of each player are updated asynchronously during the game. Two inference methods of the interactions between players are derived with naïve mean-field (nMF) approximation and maximum log-likelihood estimation (MLE), respectively. Two methods are tested numerically also for fully connected asymmetric Sherrington–Kirkpatrick models, varying the data length, asymmetric degree, payoff, and system noise (coupling strength). We find that the mean square error of reconstruction for the MLE method is inversely proportional to the data length and typically half (benefit from the extra information of update times) of that by nMF. Both methods are robust to the asymmetric degree but work better for large payoffs. Compared with MLE, nMF is more sensitive to the strength of couplings and prefers weak couplings.

Keywords: network reconstruction, prisoner's dilemma game, asynchronously update

PACS: 02.50.Tt, 02.30.Mv, 89.75.Fb, 87.10.Mn **DOI:** 10.1088/1674-1056/acc7fd

1. Introduction

Prisoner's dilemma game (PDG) has long been studied for the emergence of cooperation among connected selfish agents.[1–4] Every two criminals simultaneously take a cooperation strategy to confess a crime to the judge or a defection strategy by refusing confession. Then the players' strategies can be binarized, $+1$ for cooperation while -1 for defection. Meanwhile, networks are generally used for studying the collective behaviors in such a system composed of interacting elements, ranging from biological systems[5,6] to social science.[7–10] A large number of studies have focused on the emergence of cooperation with different network structures, e.g., small-world networks,[2,11] two-dimensional lattices,[12] scale-free networks,[13] and two-layered networks.[14]

Previous studies are typically based on a certain assumed network structure which is usually unavailable. Instead, the collective behaviors based on the time-dependent strategies of players are easier to be accessed. Thus uncovering the underlying relations between players from available observations is crucial to understand how collective behaviors emerge.

Reconstructing the couplings between elements in a network from observations is referred to as inference in statistical physics.[15] With binary observations, it is straightforward to pose the coupling inference problem to the reconstruction of an Ising model. This is known as the inverse Ising problem.[16–22] There are many related algorithms for recovering the couplings of the inverse Ising problems, as reviewed in Ref. [22] and references therein. This field has also attracted great interests in various fields, ranging from biology[23–25] to sociology.[26]

Generally, couplings can be reconstructed by equilibrium[20,27,28] or non-equilibrium[18,19,21,29,30] models given the time-independent or time-dependent data, respectively. However, in many applications, equilibrium Ising models are typically not an ideal choice for network inference and statistical modeling of the data. A mismatch between the real couplings and the inferred ones can be seen for large systems.[17,31,32] This is mainly because these systems have an out-of-equilibrium nature and asymmetric couplings between elements. Thus, researchers have moved to the kinetic Ising models, developing exact and approximate methods for network reconstruction,[19,21,31,33] which have wider generality.

With kinetic Ising models, the elements included can update synchronously or asynchronously. Similarly, with evolutionary games, synchronous means all players update their strategies simultaneously at every time step.[34] This can be mathematically described by a finite difference equation but rarely exists in social or natural systems. The players or organisms usually act at different and uncorrelated times with the coming information which may be delayed and imperfect.[35] For instance, a neuron will be in a refractory period after releasing a spike, it cannot respond to an input signal because it is still processing or recovering from the previous input signal.[36,37] The dynamics with asynchronous update is usually expressed by differential equations, whose solutions are not always the same as those of their finite-difference counter-

†Corresponding author. E-mail: smqin@cauc.edu.cn
© 2023 Chinese Physical Society and IOP Publishing Ltd

parts.

For network reconstruction with evolutionary PDG data, some methods[38,39] have been developed based on the compressive sensing technique,[40] which is a paradigm for sparse-signal reconstruction. However, the compressive sensing methodology works with assumptions that the interactions between individuals should be explicit and stationary, thus the system could be handled linearly. In Refs. [39,41,42], all agents are assumed to play the same game with a given payoff matrix and the observations are the strategies and the total payoff of each player in the game. In Refs. [43–45], the dynamical functions are employed, but they can also be decomposed into a linear sum of scalar basis functions.

In the following, we generalize the couplings between players to a fully connected asymmetric Sherrington–Kirkpatrick (aSK) model,[46] with an asymmetric degree parameter k varying between 0 (symmetric) and 1 (fully asymmetric). The couplings are assigned as Gaussian random variables and are not necessarily to be symmetric, which are closer to real systems. The exact mean-field inference in asymmetric kinetic Ising systems has been studied in Ref. [47] for both weak and strong couplings. On this aSK structure, players will update their strategies asynchronously, even though all players get their corresponding rewards through the game with and from all neighbors, only one player will update his strategy in one game round. For a finite number of players N, this is not exactly the asynchronous update described above, but we do not see any differences at least for kinetic Ising models.[19,21]

Distinct from data-driven inference methods, say, compressive sensing, etc., here we start from the dynamics and derive an exact method based on maximum-log-likelihood estimation, referred to as MLE. Moreover, an approximate inferring method is developed with naïve mean-field approximation abbreviated as nMF. Both derived inference formula for evolutionary PDG data is enlightened by the asynchronously updated Glauber dynamics,[48] which could converge to a stationary state described by the Gibbs–Boltzman distribution when the couplings are symmetric.[21] However, this is unnecessarily true for the synchronous case. Hence, we are interested in reconstructing an evolutionary game network dynamically through a kinetic Ising-like model.

With evolutionary PDG, the update times $\{\tau_i\}$, history of strategies $\{s_i(t)\}$ and rewards for each player $\{x_i(t)\}$ are the full model data generated during the game process. MLE needs all of these data while nMF does not need the update times, nor the rewards for each game round. The nMF method relies on means, correlations, and the temptation of defection parameter b in the payoff matrix. With massive numerical simulations, we find that the nMF performs very close to the MLE method while avoiding a long-time iteration process. One equilibrium inference method is also tested for the sake of completeness, which shows poor reconstruction for the couplings of our non-equilibrium processes.

The paper is organized as follows. In Section 2, we present the testing network structure as well as the dynamics for the PD evolutionary game. In Section 3, we derive the MLE and nMF inference formulae from evolutionary game data. Section 4 presents how these two methods perform for the network reconstruction. In Section 5 we summarize and discuss the results. The derivation details of the exact external fields are given in Appendix A while the nMF approximation is given in Appendix B.

2. The asymmetric SK model and Glauber-like game dynamics

The quenched aSK model is composed of N vertices representing N game players with two kinds of strategies ($s_i = 1$ for cooperation while $s_i = -1$ for defection). This is a fully connected model, i.e., all players are connected. The interactions J_{ij} between each pair of players have the form of

$$J_{ij} = J^{\rm s}_{ij} + kJ^{\rm as}_{ij}, \qquad k \geq 0, \tag{1}$$

where k is the asymmetric degree of these interactions, $J^{\rm s}_{ij} = J^{\rm s}_{ji}$ and $J^{\rm as}_{ij} = -J^{\rm as}_{ji}$ are symmetric and asymmetric matrices, respectively. They are Gaussian random variables with means 0 and variances

$$\sigma^2(J^{\rm s}_{ij}) = \sigma^2(J^{\rm as}_{ij}) = \frac{g^2}{N}\frac{1}{1+k^2}, \tag{2}$$

with g being a tunable parameter determining the coupling strength between players. The players do not play the game with themselves, which indicates $J_{ii} = 0$, and the diagonal elements of $J^{\rm s}_{ij}$ and $J^{\rm as}_{ij}$ are 0 as well. Equation (2) guarantees the variance of J_{ij} as g^2/N to be an intensive quantity.

We will describe the dynamics of the evolutionary game on the aSK network model. In an evolutionary PDG, the judge knows that the players are criminals but without evidence. Then a player has two possible strategies: cooperation (C) or defection (D). The rewards based on their strategies are a 2×2 payoff matrix with four entities corresponding to the payoff given to the "row" player. The players get rewards $R(P)$ if both choose cooperation (defection). In the other two cases, the defector's and cooperator's payoffs are T (the temptation to defect) and S (sucker's payoff), respectively. For PDG, we must have $T > R > P > S$ and $2R > T + S$.[1] For the sake of convenience, we take $R = 1$ and $S = P = 0$ while T is a tunable parameter b. Then we have the PDG payoff matrix X as follows:

$$X = \begin{array}{c} \\ {\rm C} \\ {\rm D} \end{array}\!\!\begin{array}{c} \begin{array}{cc} {\rm C} & {\rm D} \end{array} \\ \begin{pmatrix} 1 & 0 \\ b & 0 \end{pmatrix} \end{array}, \tag{3}$$

with $1 \leq b \leq 2$.

During each time step t, all players play games simultaneously and get corresponding rewards according to the payoff matrix X in Eq. (3). Thus, for each player, the rewards come from the games played as well as from the neighbors. Once they get the rewards from the game, one randomly chosen player i will be assigned to update his strategy according to the following formula:

$$P(s_i(t)) = \frac{\exp\left(\sum_j J_{ij}x_j(t-1)\delta_{s_j(t-1),s_i(t)}\right)}{Z_i(t)}. \tag{4}$$

Here, "update" means that a new strategy will be adopted by player i at time t, δ is the Kronecker delta function which will return 1 if two subscripts are the same, and 0 otherwise, $s_i(t)$ and $x_i(t)$ are the strategies chosen by player i and the consequent reward at time step t, respectively. This indicates that player i prefers to take the same strategy with its connected neighbors. Meanwhile,

$$Z_i(t) = \sum_{s_i(t)=\pm 1} \exp\left(\sum_j J_{ij}x_j(t-1)\delta_{s_j(t-1),s_i(t)}\right)$$

is the normalization factor (local partition function), which sums over cooperation and defection states of player i.

We denote the total payoff of the cooperative and defective strategy used by player i at time t as $\alpha_i(t)$ and $\beta_i(t)$, respectively,

$$\alpha_i(t) = \sum_j J_{ij}x_j(t-1)\delta_{s_j(t-1),+1}, \tag{5a}$$

$$\beta_i(t) = \sum_j J_{ij}x_j(t-1)\delta_{s_j(t-1),-1}. \tag{5b}$$

Then the partition function can be rewritten as

$$Z_i(t) = \exp[\alpha_i(t)] + \exp[\beta_i(t)]. \tag{6}$$

With the definition of

$$H_i(t) = \frac{1}{2}[\alpha_i(t) - \beta_i(t)] = \sum_j J_{ij}s_j(t-1)\frac{x_j(t-1)}{2}, \tag{7}$$

and substituting $Z_i(t)$ into Eq. (4) together with Eq. (6), we have

$$\begin{aligned} P(s_i(t)) &= \frac{\exp[\alpha_i(t)]}{\exp[\alpha_i(t)] + \exp[\beta_i(t)]} = \frac{\exp[s_i(t)H_i(t)]}{2\cosh H_i(t)} \\ &= \frac{1}{2}[1 + s_i(t)\tanh H_i(t)]. \end{aligned} \tag{8}$$

During each time step, all players join the prisoners' dilemma game and obtain the corresponding payoff according to the payoff matrix (3) from each counterpart. The averaged gain during this time step for player i is derived in Eq. (A1). However, only one of the players is going to update his strategy, which does not necessarily change his current choice. This is why we refer to this dynamics as asynchronous PDG.

3. Inferences for game networks

3.1. Maximum log-likelihood estimation

Suppose we have the following data: history of players' strategies $\boldsymbol{s} \equiv \{s_i(t)\}$, updating times $\boldsymbol{\xi} \equiv \{\xi_i\}$ and payoff of each player $\boldsymbol{x} \equiv \{x_i(t)\}$, of length $L = T \times N$ steps. We reconstruct the game network based on these data. This can be carried out by maximizing the likelihood $P(\boldsymbol{s}, \boldsymbol{\xi}, \boldsymbol{x}) = P(\boldsymbol{s}, \boldsymbol{x}|\boldsymbol{\xi})p(\boldsymbol{\xi})$ over these parameters. As mentioned in Ref. [21] for each player i, the chance of updating their strategy is a Poisson process. This indicates that the probability of the update history $p(\boldsymbol{\xi})$ is independent of the model parameters, thus we can take the objective function as $\log P(\boldsymbol{s}, \boldsymbol{x}|\boldsymbol{\xi})$ safely from Eq. (8) taking a time discretization with a step size of δt,

$$\mathcal{L} = \sum_i \sum_{\xi_i} [s_i(\xi_i + \delta t)H_i(\xi_i) - \log 2\cosh H_i(\xi_i)]. \tag{9}$$

The sum is only over the update times instead of all time steps as in the synchronous case.[31] Then it leads to a learning rule for couplings J_{ij},

$$\delta J_{ij} \propto \frac{\partial \mathcal{L}}{\partial J_{ij}} \propto \sum_{\xi_i} [s_i(\xi_i + \delta t) - \tanh H_i(\xi_i)]s_j(\tau_i)\frac{x_j(\xi_i)}{2}. \tag{10}$$

We refer to this algorithm as "MLE". It is an exact method as no approximation is introduced to the derivation of the inference formula. In addition, it is notable that if the rewards for each player are equal to 2 and the same as each other, then the PDG process will degenerate to the original Glauber dynamics.[48]

3.2. Naïve mean field approximation

We start with the master equation

$$\begin{aligned} \frac{\mathrm{d}p(\boldsymbol{S};t)}{\mathrm{d}t} &= \sum_i \omega_i(-s_i(t))p(s_1, ..., -s_i, ...s_N; t) \\ &\quad - \sum_i \omega_i(s_i(t))p(\boldsymbol{S};t), \end{aligned} \tag{11}$$

and the flipping rate is

$$\omega_i(\boldsymbol{S};t) = \frac{1}{2}[1 - s_i(t)\tanh H_i(t)], \tag{12}$$

which could be obtained by the following detailed balanced condition:[49]

$$\frac{p(-s_i)}{p(s_i)} = \frac{\omega(s_i)}{\omega(-s_i)}, \tag{13a}$$

$$p(-s_i) + p(s_i) = 1. \tag{13b}$$

With strategy history for each player $\{s_i(t)\}$, the time-dependent means and correlations can be defined as

$$m_i(t) = \langle s_i(t)\rangle, \tag{14a}$$

$$C_{ij}(t - t_0) = \langle s_i(t)s_j(t_0)\rangle - m_i(t)m_j(t). \tag{14b}$$

From Eqs. (11) and (12), the temporal behavior of means and correlations reads

$$\frac{\mathrm{d}m_i(t)}{\mathrm{d}t} = -m_i(t) + \langle \tanh[H_i(t)] \rangle, \tag{15a}$$

$$\frac{\mathrm{d}\langle s_i(t)s_j(t_0)\rangle}{\mathrm{d}t} = -\langle s_i(t)s_j(t_0)\rangle + \langle \tanh[H_i(t)]s_j(t_0)\rangle. \tag{15b}$$

Thus, the external field (influence) $H_i(t)$ for player i at time t in Eq. (7) could be rewritten as

$$H_i(t) = \sum_j J_{ij}s_j(t)x_j(t) = \sum_j J_{ij}(B_0 + B_1 s_j(t-1)), \tag{16}$$

where $B_0 = (1-b)(1+\bar{m}(t))/4$ and $B_1 = (1+b)(1+\bar{m}(t))/4$ are two non-fluctuating terms depending on parameter b and $\bar{m}(t)$, with $\bar{m}(t) = \frac{1}{N}\sum_i s_i(t)$ being the population average. The detailed derivation of Eq. (16) is shown in Appendix A.

The nMF approximation hence is formally the same as that of the original asynchronously updated kinetic Ising model in Ref. [19],

$$m_i = \tanh b_i, \tag{17}$$

but with

$$b_i = \sum_{j\in\partial i} J_{ij}(B_0 + B_1 m_j), \tag{18}$$

which is obtained by taking the stationary solution of Eq. (15a) with the naïve mean field approximation. The details are illustrated in Appendix B.

With the time derivative of correlations in Eq. (15b), the tanh function can be expanded with respect to b_i, yielding

$$\begin{aligned}&\frac{\mathrm{d}}{\mathrm{d}t}\langle s_i(t)s_j(t_0)\rangle + \langle s_i(t)s_j(t_0)\rangle \\ =&m_i m_j + B_1(1-m_i^2)\sum_k J_{ik}\langle \delta s_k(t)\delta s_j(t_0)\rangle.\end{aligned} \tag{19}$$

Denoting $\tau = t - t_0$, we obtain

$$\frac{\mathrm{d}}{\mathrm{d}\tau}C_{ij}(\tau) + C_{ij}(\tau) = B_1(1-m_i^2)\sum_k J_{ik}C_{kj}(\tau). \tag{20}$$

With the limit $\tau \to 0$, we can obtain the nMF inference formula for the PDG network as follows:

$$J = \frac{A^{-1}DC^{-1}}{B_1}, \tag{21}$$

with $D = \dot{C}(0) + C(0)$, $A_{ij} = \delta_{ij}(1-m_i^2)$, and $B_1 = (1+b)(\bar{m}+1)/4$. With full data history, it is safe to replace $\bar{m}(t)$ with the time average $\bar{m} = \langle \bar{m}(t)\rangle_t$.

4. Numerical results

We infer the evolutionary game network by MLE (10) and nMF (21) formulas, respectively. In Fig. 1, the scatter plots for the reconstructed structure against the true ones are presented for both the methods. Figure 1(a) is for the data length $L = N \times 10^5$ and Fig. 1(b) for $L = N \times 10^7$. It shows that both nMF and MLE perform better with larger data lengths L. Furthermore, MLE works slightly better than nMF in both the cases. The nMF method overestimates the couplings especially for $L = N \times 10^7$, as shown in Fig. 1(b).

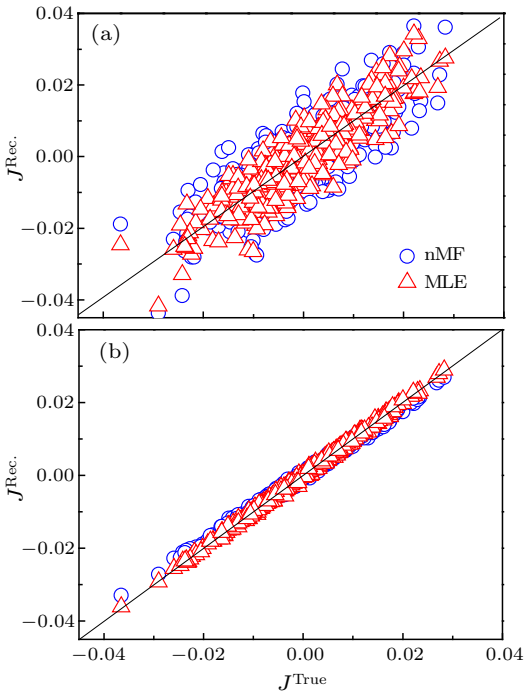


Fig. 1. Scatter plots for reconstructed couplings versus the tested ones with different data lengths L: (a) $L = N \times 10^5$, (b) $L = N \times 10^7$. Blue open dots are recovered couplings by nMF while open red upper triangles are for MLE. The other parameters are taken as follows: the number of players $N = 20$, asymmetric degree $k = 1$, and coupling strength $g = 0.3$.

We introduce the mean square error (MSE) to measure the distance between the reconstructed and the tested network structure,

$$\mathrm{MSE} = \frac{\sum_{ij}(J_{ij}^{\mathrm{Rec.}} - J_{ij}^{\mathrm{True}})^2}{N(N-1)}, \tag{22}$$

where J_{ij}^{True} represents the tested network couplings, and $J_{ij}^{\mathrm{Rec.}}$ denotes the inferred ones.

With the MSE defined by Eq. (22), we compare the performance of the MLE and nMF methods for fully connected SK models (1). We study both the methods for different data lengths L, the asymmetric degree k, the temptation of defection parameter b in the payoff matrix (3) as well as the coupling strength g. The inverse of g corresponds to the temperature in the spin glass system, which can be explained as the noise (say, fake information or rumors etcetera) in the evolutionary PDG.

Figure 2 shows the performance of both the methods. Similar to the results for the asynchronous Ising case,[21] the MSE for MLE is $\propto 1/L$ here. However, with the data length L

we tested here, nMF does not approach to a saturated value as happened for the asynchronous Ising case. Instead, the MSE for nMF is about twice that of MLE, see Fig. 2(a). This could be an indication for the game network, nMF inference formula can also be obtained by taking the average of update times in the MLE formula (10), which has been proved in Ref. [21] for asynchronous Ising models. Figure 2(b) shows that the MSE for both the methods is insensitive to the asymmetric degree k, no matter whether the network is symmetric ($k = 0$) or fully asymmetric ($k = 1$). Here, the data length $L = N \times 10^6$ with $N = 20$ and $g = 0.3$. The difference between the two methods is affected mainly by the data length L. The MSE for MLE is about half the value for the nMF approach, which agrees well with that shown in Fig. 2(a). Figure 2(c) shows the performance of MLE and nMF algorithm for different reward parameters b in the payoff matrix (3), which is a specific parameter for game networks. Both algorithms recover the network better with larger reward b. However, the proportion of MSE between nMF and MLE increases slightly for larger b. Finally, the effects of inverse g over network inference are illustrated in Fig. 2(d). For strong couplings, nMF works much worse than MLE. However, for $g \leq 1$, their performances are not affected by g anymore. MLE still has its advantage of factor 2 (conferred by the information of update times) compared with nMF.

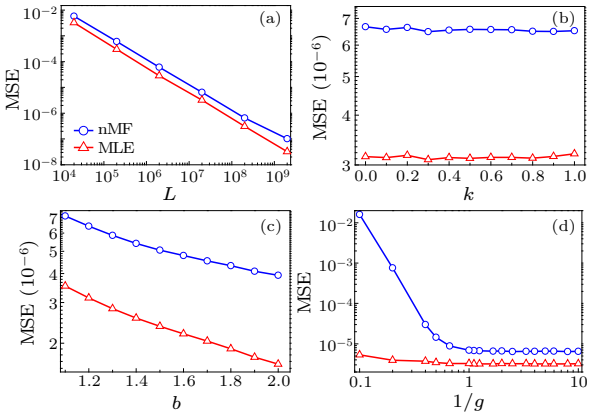


Fig. 2. Mean square error (MSE) for (a) data length L, (b) asymmetric degree k, (c) b parameter in the payoff matrix, and (d) temperature $1/g$. Blue open dots are for the nMF while red solid dots are for the MLE. The parameters are $N = 20$, $L = N \times 10^6$, $k = 1$, and $g = 0.3$, except the varying parameters in the corresponding panels.

To check if there is a critical value of $1/g$ that depends on the value of k, the phase diagram of the reconstruction error for nMF (left panel) and MLE (right panel) is plotted in Fig. 3. It is shown that the critical value of $1/g$ for both nMF and MLE seems independent of k. The nMF works much worse with strong couplings than the MLE method. Meanwhile, both of them work poorly for the symmetric case with $k = 0$ compared with themselves.

To illustrate how the equilibrium inference method works for the non-equilibrium process, we use the naïve mean-filed equilibrium inference[16] algorithm, which depends on the equal time correlations only, i.e.,

$$J^{\text{Equi}} = -C^{-1}. \tag{23}$$

We refer to this as the equilibrium inference to avoid confusion with the nMF method for the asynchronous case derived here. Then, we present the inferred networks through scatter plots in Fig. 4 with both equilibrium and non-equilibrium methods for evolutionary data generated by PDGs.

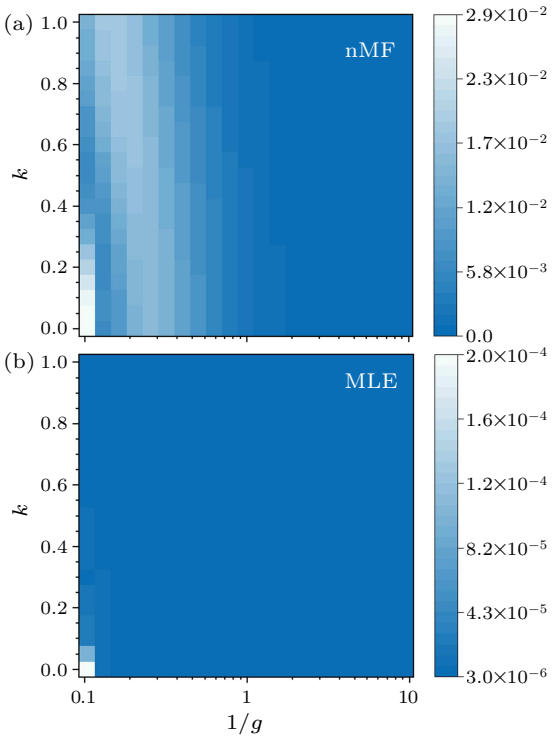


Fig. 3. Phase diagram of reconstruction error with parameters k and coupling strength g. The nMF method works poorly at strong couplings or low temperatures while the MLE performs much better than the nMF. Meanwhile, both the nMF and MLE methods show poor reconstruction at strong couplings for the symmetric case $k = 0$ compared to themselves.

Figures 4(a) and 4(b) present the reconstructed couplings for the symmetric ($k = 0$) and fully asymmetric ($k = 1$) SK models, respectively. Our asynchronous nMF (blue open dots) and MLE (red upper triangle) methods recover the couplings nicely while the equilibrium nMF (23) (open black squares) works much worse, even for $k = 0$, the symmetric case. It is unsurprising that the equilibrium nMF (23) we tested here does not take into account the game process at all. For the original asynchronous Ising model without a game process, the equilibrium nMF should work as good as the non-equilibrium methods[32] since they are for the same dynamics.

5. Discussion and conclusion

We reconstruct the game network with data produced by an asynchronously updated evolutionary game. The gamblers play the PDG with their counterparts simultaneously but update their strategies asynchronously. Two methods (exact and

iterative MLE and approximate nMF) are introduced to infer the fully connected and Gaussian-distributed couplings between players.

Compared with the original asynchronous Ising model,[19,21] we combine the PDGs with Glauber dynamics, where the rewards during the game for each player are considered. The MLE and nMF reconstruction formulae for the asynchronous Ising models in Refs. [19,21] hence must be generalized for the asynchronous evolutionary game case here. MLE is derived from the log-likelihood of the system while nMF is from the derivative of the equations of motion of means and correlations. Nevertheless, they are interrelated with each other. MLE utilizes the full model histories, $\{s_i(t)\}$, $\{x_i(t)\}$, and $\{\xi_i\}$. The update histories in Eq. (10) could be averaged, and the nMF inference formula (21) is yielded by taking the linear term of the averaged tanh function.

With the derived MLE and nMF methods for asynchronous updates PDG, our numerical results show that the inference performance of nMF is comparable with that of MLE. Both the methods are not sensitive to the asymmetric degree k, but proportional to the inverse of data length. For fixed data length, the reconstruction error (MSE) of MLE is half (benefit from update times) the error by the nMF method. Furthermore, nMF prefers weak coupling strength (g) while MLE holds for a much wider range of g. Both the methods recover better for large payoff parameters b. This is reasonable as the rewards of each player equal 2, then the external field Eq. (7) in the dynamics degenerates to the original asynchronous Ising model. With b increasing, the rewards of each player will also be close to 2, which shows better performance of network reconstruction.

However, compared with the data that the MLE method used for inference, nMF needs only the b parameter and the moments of strategy history $\{s_i(t)\}$. Furthermore, nMF infers much fast than MLE as no iterative procedure is included for network inference. The scatter plots in Figs. 1 and 4 show that the J_{ij}^{nMF} is comparable with J_{ij}^{MLE}, even though the MSE for nMF is roughly twice that for MLE. Thus, we expect that for the network inference with data from asynchronous PDG, nMF works well enough. One can further consider higher orders of J_{ij} in the tanh function during the expansion process to get a Thouless–Anderson–Palmer (TAP) version of the inference for the PDG network. However, according to Fig. 4 shown in Ref. [19], the difference between nMF and TAP is only available with a large amount of data. Thus we believe that nMF would have wider applications compared with TAP.

Furthermore, we have tested a widely used equilibrium inference method (23) blindly for our dynamic data generated from evolutionary PDGs, which recover much worse than that by non-equilibrium inference methods, even for symmetric interactions between players, as illustrated in Fig. 4(a). This implies that if we have time series data generated from certain dynamics, we should try non-equilibrium methods first. Furthermore, we start from the detailed balance condition to derive the asynchronous nMF formula for the network inference, but as shown by the numerical results, the inference formula also holds for the asymmetric $k = 1$ case in which the system is not in the equilibrium realm anymore.

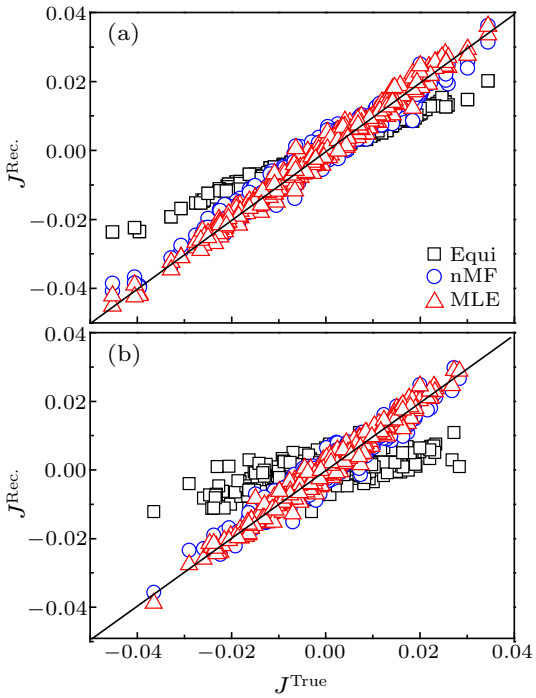


Fig. 4. Scatter plot for recovered links with the tested ones for different asymmetric degrees k: (a) asymmetric degree $k = 0$, symmetric SK model, (b) $k = 1$, fully asymmetric SK model. Black open squares are for inferred couplings with equilibrium inference $J^{\mathrm{Equi}} = -C(0)^{-1}$. Blue open dots are for asynchronous nMF while red open triangles are for MLE. The other parameters are taken as the data length $L = N \times 10^6$, number of players $N = 20$, and coupling strength $g = 0.3$.

This work focuses on a simple and idealized prisoner's game with fully connected and Gaussian-distributed interactions. It is convenient for the application of mean-field theory. However, the L_1 regularizations could be applied to the objective function in Eq. (9) to remove the spurious weak couplings between players.[50] Meanwhile, the connections between players could be extended to certain structures or different distributions (say, random power law, where there are strong couplings between a few players while weak ones between most of them) for the couplings. Moreover, we use a constant value of defection temptation b, which could differ for each player. Meanwhile, nonzero abut small r in the payoff matrix (3) could also be tested. These will be studied by further work.

Appendix A: Reformulating the external field

According to the PDG payoff matrix (3), the average reward player i will gain at time t is (for simplicity, r is assumed

to be equal to 0)

$$x_i(t) = 2\times\Big\{\frac{1+s_i(t)}{2}\frac{1}{N}\sum_{j\in\partial i}\frac{1+s_j(t)}{2} + \frac{1-s_i(t)}{2}\frac{b}{N}\sum_{j\in\partial i}\frac{1+s_j(t)}{2}\Big\}. \tag{A1}$$

The factor 2 outside the bracket comes from the fact that players obtained rewards from the game with neighbors as well as the games originated from neighbors within each time step of synchronous PDGs. Then $s_i(t)\frac{x_i(t)}{2}$ in Eq. (7) is

$$s_i(t)\frac{x_i(t)}{2} = \frac{s_i(t)+1}{2}f(c) + \frac{s_i(t)-1}{2}bf(c), \tag{A2}$$

with $f(c)$ being the cooperation density in the neighborhood of player i, i.e.,

$$f(c) = \frac{1}{N}\sum_{j\in\partial i}\frac{1+s_j(t)}{2} = \frac{\bar{m}(t)+1}{2}. \tag{A3}$$

Hence, we rewrite Eq. (A2) as

$$s_i(t)\frac{x_i(t)}{2} = B_0 + B_1 s_i(t), \tag{A4}$$

with

$$B_0 = \frac{1-b}{2}f(c) = \frac{(1-b)[\bar{m}(t)+1]}{4}, \tag{A5a}$$

$$B_1 = \frac{1+b}{2}f(c) = \frac{(1+b)[\bar{m}(t)+1]}{4}, \tag{A5b}$$

and $\bar{m}(t) = \frac{1}{N}\sum_i s_i(t)$.

Thus, we reformulate Eq. (7) as

$$H_i(t) = \sum_j J_{ij}[B_0 + B_1 s_j(t-1)]. \tag{A6}$$

Appendix B: nMF approximation

Substituting $s_j(t-1)$ with non-fluctuating and fluctuating terms as

$$H_i(t) = \sum_j J_{ij}(B_0 + B_1(m_j + \delta s_j(t-1))), \tag{B1}$$

and define

$$b_i = \sum_j J_{ij}(B_0 + B_1 m_j), \tag{B2}$$

then

$$\langle\tanh[H_i(t)]\rangle = \Big\langle \tanh\Big[b_i + B_1\sum_j J_{ij}\delta s_j(t-1)\Big]\Big\rangle, \tag{B3}$$

expanding the tanh function with respect to b_i to the first order, we get

$$\langle\tanh[H_i(t)]\rangle = \tanh b_i + B_1(1-\tanh^2 b_i)\Big\langle\sum_j J_{ij}\delta s_j(t-1)\Big\rangle, \tag{B4}$$

where the second term on the right-hand side goes to zero. Hence, we have the naïve mean-field approximation for m_i as follows:

$$m_i = \tanh b_i, \tag{B5}$$

which is the stationary solution of the time derivative of magnetization in Eq. (15a).

Acknowledgments

We sincerely thank John Hertz, Erik Aurell, and Pan Zhang for heuristic and fruitful discussions and suggestions. This work was supported by the National Natural Science Foundation of China (Grant Nos. 11705079 and 11705279), the Scientific Research Foundation of Nanjing University of Posts and Telecommunications (Grant Nos. NY221101 and NY222134), and the Science and Technology Innovation Training Program (Grant No. STITP_202210293044Z).

References

[1] Axelrod R and Hamilton W D 1981 *Science* **211** 1390
[2] Abramson G and Kuperman M 2001 *Phys. Rev. E* **63** 030901
[3] Santos F C, Pacheco J M and Lenaerts T 2006 *Proc. Natl. Acad. Sci. USA* **103** 3490
[4] Cressman R and Tao Y 2014 *Proc. Natl. Acad. Sci. USA* **111** 10810
[5] Adami C, Schossau J and Hintze A 2016 *Phys. Life Rev.* **19** 1
[6] Gosak M, Markovič R, Dolenšek J, Rupnik M S, Marhl M, Stožer A and Perc M 2018 *Phys. Life Rev.* **24** 118
[7] Perc M, Jordan J J, Rand D G, Wang Z, Boccaletti S and Szolnoki A 2017 *Phys. Rep.* **687** 1
[8] Wang Z, Jusup M, Shi L, Lee J H, Iwasa Y and Boccaletti S 2018 *Nat. Commun.* **9** 2954
[9] Mao Y, Rong Z and Wu Z X 2021 *Appl. Math. Comput.* **392** 125679
[10] Cui W, Xiao J, Li T and Xu X 2019 *Chin. Phys. B* **28** 068901
[11] Masuda N and Aihara K 2003 *Phys. Lett. A* **313** 55
[12] Szabó G and Töke C 1998 *Phys. Rev. E* **58** 69
[13] Chen Y S, Lin H and Wu C X 2007 *Physica A* **385** 379
[14] Li D D, Du J G and Han D 2019 *Europhys. Lett.* **126** 30002
[15] Lai D, Shu X and Nardini C 2017 *Chin. Phys. B* **26** 038902
[16] Kappen H J and Spanjers J J 2000 *Phys. Rev. E* **61** 5658
[17] Roudi Y, Nirenberg S and Latham P E 2009 *PLoS Comput. Biol.* **5** e1000380
[18] Roudi Y and Hertz J 2011 *Phys. Rev. Lett.* **106** 048702
[19] Zeng H L, Aurell E, Alava M and Mahmoudi H 2011 *Phys. Rev. E* **83** 041135
[20] Aurell E and Ekeberg M 2012 *Phys. Rev. Lett.* **108** 090201
[21] Zeng H L, Alava M, Aurell E, Hertz J and Roudi Y 2013 *Phys. Rev. Lett.* **110** 210601
[22] Nguyen H C, Zecchina R and Berg J 2017 *Adv. Phys.* **66** 197
[23] Zeng H L and Aurell E 2020 *Phys. Rev. E* **101** 052409
[24] Zeng H L, Dichio V, Rodríguez Horta E, Thorell K and Aurell E 2020 *Proc. Natl. Acad. Sci. USA* **117** 31519
[25] Zeng H L, Mauri E, Dichio V, Cocco S, Monasson R and Aurell E 2021 *J. Stat. Mech.: Theory Exp.* **2021** 083501
[26] Zeng H L, Lemoy R and Alava M 2014 *J. Stat. Mech.: Theory Exp.* **2014** P07008
[27] Cocco S, Leibler S and Monasson R 2009 *Proc. Natl. Acad. Sci. USA* **106** 14058
[28] Weigt M, White R A, Szurmant H, Hoch J A and Hwa T 2009 *Proc. Natl. Acad. Sci. USA* **106** 67
[29] Pillow J W, Shlens J, Paninski L, Sher A, Litke A M, Chichilnisky E and Simoncelli E P 2008 *Nature* **454** 995
[30] Zhang P 2012 *J. Stat. Phys.* **148** 502
[31] Roudi Y and Hertz J 2011 *Phys. Rev. Lett.* **106** 048702

[32] Zeng H L and Aurell E 2020 *Chin. Phys. B* **29** 080201
[33] Cocco S, Leibler S and Monasson R 2009 *Proc. Natl. Acad. Sci. USA* **106** 14058
[34] Nowak M A and May R M 1992 *Nature* **359** 826
[35] Huberman B A and Glance N S 1993 *Proc. Natl. Acad. Sci. USA* **90** 7716
[36] Greil F, Drossel B and Sattler J 2007 *New J. Phys.* **9** 373
[37] Zeng H L, Zhu C P, Wang S X, Guo Y D, Gu Z M and Hu C K 2020 *Physica A* **540** 123191
[38] Wang W X, Lai Y C and Grebogi C 2016 *Phys. Rep.* **644** 1
[39] Wang W X, Lai Y C, Grebogi C and Ye J 2011 *Phys. Rev. X* **1** 021021
[40] Foucart S and Rauhut H 2013 *An Invitation to Compressive Sensing.* In: *A Mathematical Introduction to Compressive Sensing. Applied and Numerical Harmonic Analysis* (New York: Birkhäuser) Vol. 54 p 151
[41] Guo Q, Liang G, Fu J Q, Han J T and Liu J G 2016 *Phys. Rev. E* **94** 052303
[42] Wu K, Liu J and Wang S 2016 *Sci. Rep.* **6** 37771
[43] Steinke F, Seeger M and Tsuda K 2007 *BMC Syst. Biol.* **1** 51
[44] Chang Y H, Gray J W and Tomlin C J 2014 *BMC Bioinform.* **15** 400
[45] Li J, Shen Z, Wang W X, Grebogi C and Lai Y C 2017 *Phys. Rev. E* **95** 032303
[46] Kirkpatrick S and Sherrington D 1978 *Phys. Rev. B* **17** 4384
[47] Mézard M and Sakellariou J 2011 *J. Stat. Mech.: Theory Exp.* **2011** L07001
[48] Glauber R J 1963 *J. Math. Phys.* **4** 294
[49] Van Kampen N G 1992 *Stochastic Processes in Physics and Chemistry* (Amsterdam: Elsevier) Vol. 1
[50] Zeng H L, Hertz J and Roudi Y 2014 *Phys. Scr.* **89** 105002